

## Three-dimensional image reconstruction from ordered arrays of 70S ribosomes

T. ARAD<sup>1</sup>, J. PIEFKE<sup>2</sup>, S. WEINSTEIN<sup>1</sup>, H.-S. GEWITZ<sup>2</sup>, A. YONATH<sup>1,3</sup> and H.G. WITTMANN<sup>2,\*</sup>

<sup>1</sup>Weizmann Institute of Science, Rehovot, Israel

<sup>2</sup>Max Planck Institut für Molekulare Genetik, Ihnestrasse 73, D-1000 Berlin 33, FRG

<sup>3</sup>Max Planck Research Unit for Structural Molecular Biology, D-2000 Hamburg, FRG

(Received 8-4-1987, accepted after revision 26-5-1987)

**Summary** – A better understanding of the molecular mechanism of protein biosynthesis still awaits a reliable model for the ribosomal particle. We describe here the application of a diffraction technique, namely three-dimensional image reconstruction from two-dimensional sheets of 70S ribosomes from *Bacillus stearothermophilus* at 47 Å resolution. The three-dimensional model obtained by these studies shows clearly the two subunits, the contact points between them, an empty space large enough to accommodate the components of protein biosynthesis, the location of regions rich in RNA and a possible binding site for mRNA. The tunnel within the 50S particle which may provide the path taken by the nascent polypeptide chain in partially resolved.

**70S ribosomes / *Bacillus stearothermophilus* / three-dimensional image reconstruction**

**Résumé** – **Reconstruction de l'image à trois dimensions des strates structurées des ribosomes 70S.**

*Pour mieux comprendre le mécanisme moléculaire de la biosynthèse protéique il est encore nécessaire de développer un modèle solide de la particule ribosomale.*

*Nous présentons ici l'application d'une technique de diffraction, c'est-à-dire la reconstruction de l'image à trois dimensions des strates à deux dimensions des ribosomes 70S du *Bacillus stearothermophilus* d'une résolution de 47 Å.*

*Le modèle à trois dimensions obtenu par ces recherches montre clairement les deux sous-unités, les points de contact entre elles, un endroit vide mais assez large à accommoder les composants de la biosynthèse protéique, la position des endroits riches en ARN et un lieu d'interaction possible de mRNA. Le tunnel à travers la particule 50S qui pourrait fournir le chemin pris par la chaîne polypeptidique croissante est partiellement visible.*

**ribosomes 70S / *Bacillus stearothermophilus* / reconstruction de l'image à trois dimensions**

### Introduction

The key role of ribosomes in protein biosynthesis stimulated us to initiate structural studies by diffraction method. We have developed an *in vitro*

crystallization procedure for intact ribosomal particles from bacterial sources. Three-dimensional crystals of the large ribosomal subunits from *Halo-bacterium marismortui* [1] and *Bacillus stearothermophilus* [2-5] diffracting X-rays to 5.5 Å and

\* To whom correspondence should be addressed.

13 Å, respectively, were obtained. From the latter species it was also possible to grow two types of well ordered two-dimensional crystalline sheets: using alcohols [6], and salt mixtures (T. Arad, J. Piefke *et al.*, submitted). Attempts to grow periodically packed objects from whole ribosomes resulted in the growth of micro three-dimensional crystals of ribosomes from *E. coli* [7] and two-dimensional sheets of ribosomes from *B. stearothermophilus* [8]. Both systems are very well packed, but until recently these objects have been too small for the application of diffraction studies at reasonable resolution.

Our newly developed method (T. Arad, J. Piefke *et al.*, submitted) for growth of two-dimensional sheets using mixtures of salts and alcohols have recently been improved, and currently we are able to produce large sheets of the 50S subunits and the 70S ribosomes from *B. stearothermophilus*. These have been proved to be suitable for three-dimensional image reconstruction studies. Such studies, performed on the sheets of the 50S subunits at 30 Å resolution have already revealed a tunnel which spans these particles and may provide the path of the growing nascent polypeptide chain [9].

Here we describe the results of three-dimensional image reconstruction studies on two-dimensional sheets of 70S ribosomes from *B. stearothermophilus* negatively stained by gold-thioglucose as well as by uranyl acetate. Although the resolution limit of these sheets is not as high as that of the sheets from the 50S subunits, the resulting model shows interesting features such as a wide separation between the two subunits and the location of RNA rich regions. There is also evidence for the existence of a tunnel similar to that which has been detected in the reconstruction of the large ribosomal subunits [9].

## Materials and methods

### *Production of two-dimensional sheets*

Ribosomes were prepared and their integrity was checked as described (T. Arad, J. Piefke *et al.*, submitted).

Two-dimensional sheets have been grown and applied to electron microscope grids as described (T. Arad, J. Piefke *et al.*, submitted) and [8]. Crystallization mixtures (7–10 µl) were applied to the plastic side of carbon-coated nitrocellulose grids. These were consequently either stained for 10 s with 1% (w/v) uranyl acetate or cross-linked with 1% glutaraldehyde for 5 min and stained with 1% gold-thioglucose. Excess liquid was then removed by blotting off. The grids were examined with a 400T Phillips electron microscope, operating at 80 kV, at an electron optical magnification of  $\times 28\,000$ . Opti-

cal diffractograms were used for the determination of unit cell dimensions and resolution limits. Areas for three-dimensional image reconstruction were chosen by the criteria of the highest resolution and sharpest reflections in the optical diffraction patterns.

### *Three-dimensional image reconstruction*

Images were recorded at a dose of about 10 electrons/Å<sup>2</sup>, of the specimens tilted at angles up to  $\pm 60^\circ$ , at intervals of  $5^\circ$ , with respect to the incident electron beam. A typical tilt series contained 23 images of which the first, middle and last images were untilted. This was essential for establishing that the specimen was not severely damaged by the electron beam during recording of the tilt series. No differences have been detected between the diffraction patterns of the untilted views taken at all stages of the experiment. The images were analyzed by standard methods [10], as described previously [11]. Ordered areas in the images were selected by optical diffraction and scanned with an Optronics-1000 microdensitometer with a 25 micron raster, corresponding to 9 Å at the specimen. All computational steps were carried out on a VAX 11/780. For Fourier transforms, optical densities of arrays (512  $\times$  512) were used, and reciprocal lattices were fitted to the calculated diffraction patterns. Amplitudes and phases were extracted from peaks of at least two-standard deviations above background. Images of untilted sheets were used for the initial data in the three-dimensional analysis. The data were combined with a comparison range in  $z^*$  of  $0.0016 \text{ \AA}^{-1}$ . The average phase error for each image based on a cumulative comparison of individual phases was  $20\text{--}30^\circ$ . Each lattice line was sampled at regular intervals of  $1/300 \text{ \AA}^{-1}$  along smooth curves fitted manually to the experimental values to provide terms for the Fourier synthesis. Terms along the 0,0 lattice line were not included. Fourier synthesis of 130–300 terms yielded the three-dimensional maps. For each reconstruction we have used 2–4 complete tilt series obtained from two-dimensional sheets. Two of these tilt series were perpendicular to each other. 20–25 crystallographically independent lattice lines were extracted for each reconstruction.

### *Presentation of the model*

The three-dimensional maps were contoured either on a Textronics terminal (using the EMBL contour package) or displayed on a Vector General screen. Contour level for the particle boundary was chosen to be that at which the interparticle contacts could be resolved. For real-time display we used the computer program FRODO [12] combined with GHC650 (written by G.H. Cohen, NIH) for Fourier synthesis, and FRODOMAP (written by J.L. Bhat, NIH).

## Results and discussion

The two-dimensional sheets of 70S particles from *Bacillus stearothermophilus* consist of relatively small unit cells:  $190 \pm 15 \times 420 \pm 15 \text{ \AA}$ ,  $\gamma = 107^\circ \pm 3^\circ$

(Fig. 1). Optical diffraction patterns of electron micrographs of negatively stained specimens with uranyl acetate extend to 40 Å at best. Attempts to stain the sheets with gold-thioglucose resulted in their destruction. Therefore, they have been cross-linked with about 1% glutaraldehyde prior to staining. This procedure caused a loss of internal order,

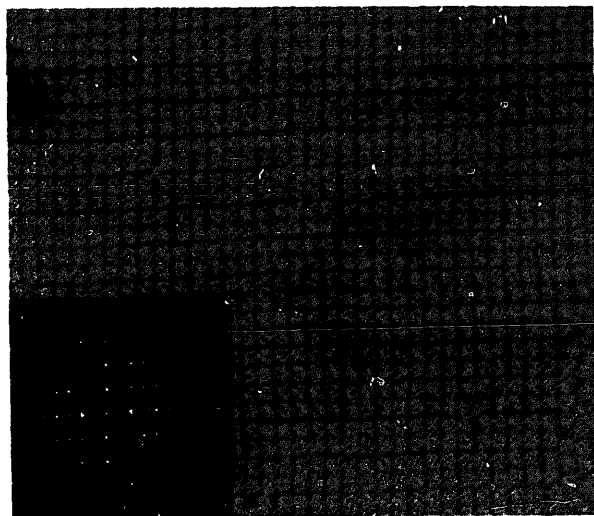


Fig. 1. Image of a two-dimensional sheet ( $\times 28\,000$ ) of 70S particles from *B. stearothermophilus* stained by uranyl acetate, and an optical diffraction pattern from a single crystalline domain containing about  $20 \times 10$  unit cells.

and negatively stained crosslinked sheets (with gold-thioglucose) diffracted to 47 Å resolution.

Each unit cell in the sheets consists of two particles with dimensions similar to those obtained by other methods [13]. Dimers have also been found within the non-crystallized material in the vicinity of the ordered sheets. Thus, they may represent the building units of the sheets. Nevertheless, three-dimensional image reconstructions were carried out assuming  $p1$  symmetry. It was found that in all reconstructions, the two particles in the unit cell are clearly resolved and show the same essential features.

We have investigated sheets from three different preparations of ribosomes. Because only a small fraction of the particles in the drop actually consists of two-dimensional sheets we could not separate them from the rest of the drop. Therefore, we tested the migration profile on sucrose gradients of the ribosomal particles in the crystallizing drops. It was found that particles subjected to crystallization conditions comigrate with standard particles (data not shown).

We have performed eleven reconstructions and investigated 22 independently reconstructed particles. The resulting model of the ribosomal particle (Fig. 2) has average dimensions similar to those determined by other physical methods [13]. The reconstructed volume ( $2.8 \times 10^6 \text{ \AA}^3$ ) corresponds to about 90% of the whole particle. On the basis

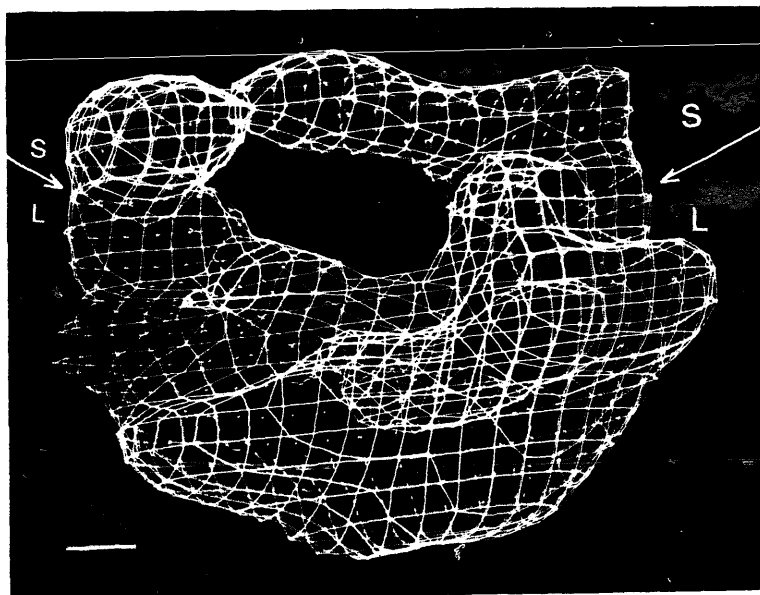


Fig. 2. Computer graphic display of the outline of the reconstructed model of the 70S ribosomal subunits at 47 Å resolution, obtained from cross-linked sheets, stained with gold-thioglucose. Bar length = 20 Å. The contact areas between the large (50S) and the small (30S) subunits are marked.

of the known molecular weight of the 70S particles ( $2.3 \times 10^6$ ) and of the volume obtained from the three-dimensional image reconstruction, the calculated density of the particle is  $1.3\text{--}1.4 \text{ g/cm}^3$ , and the  $V_m$  for a hypothetical crystal of a thickness of the sheets (about  $200 \text{ \AA}$ ) is  $2.6\text{--}2.7 \text{ \AA}^3/\text{Da}$ . These values are in good agreement with those tabulated by Matthews [14] and calculated for other large nucleoprotein structures [15, 16].

Several features were revealed by the analysis (Fig. 2) of the gold-thioglucose stained sheets. The two ribosomal subunits are arranged around an empty space of volume of up to  $4 \times 10^5 \pm 2 \times 10^5 \text{ \AA}^3$ . This space is of dimensions which are large enough to accommodate most of the components of protein biosynthesis. There are variations in the size of this space as revealed in different reconstructions. This may result from sheets, built of ribosomes which carry some components of protein biosynthesis, such as tRNA or fractions of mRNA.

Since the ribosomes were harvested in the early log phase (T. Arad, J. Piefke *et al.*, submitted) and since no attempts were made to remove the nascent polypeptide chain, the tunnel which provides the path for this chain [9] may be partially filled. In fact, compared to the case of the 50S particles, here the tunnel is only partially resolved, and evidence for its existence has been obtained by investigating sections through reconstructed particles (Fig. 3).

The two ribosomal subunits are fairly separated. Only the two ends of the small subunit are in contact with the large one. The sum of the contact areas is  $400\text{--}800 \text{ \AA}^2$ . The overall shapes of both sub-

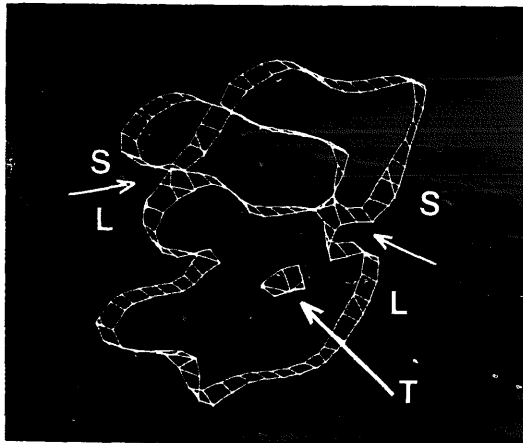


Fig. 3. A section of  $20 \text{ \AA}$  thickness of the middle of the reconstructed particle. The two subunits are resolved, and part of the tunnel (T) can be seen.

nits have been compared with models which have previously been suggested for these particles. In general, there is a similarity between the model of the small subunit obtained by visualization of single particles [13] and that revealed by our studies. The main differences are in the relative length and thickness. Isolated 30S particles seem to be shorter and wider than the reconstructed ones within the 70S particles. This may be a consequence of the contact of the isolated particles with the flat electron microscope grids. In contrast, particles within the crystalline sheets are held together by their interactions with the 50S particles as well as by interparticle crystalline forces. These construct a network which may stabilize the conformation of the particles and decrease, or even eliminate, the influence of the flatness of the grids. The portion of the reconstructed 70S particle which we assigned as the large subunit, may be correlated to the image of this subunit as revealed in our previous studies (Fig. 4 and [9]) both at  $28 \text{ \AA}$  (the actual resolution of the studies) and at  $55 \text{ \AA}$ .

We have also reconstructed models from sheets stained with uranyl acetate. The arrays used for these studies were large, stable in the electron beam and well ordered. Unlike gold-thioglucose, which is a truly negative stain, uranyl acetate functions also as a positive stain since it may interact with selected portions of the object. In the case of ribosomes the most likely candidates are RNA chains. The interaction of uranyl acetate with the particles depends on the accessibility of RNA regions. Nevertheless, in our reconstructed models derived by staining with uranyl acetate the essential features of the models obtained from sheets stained with gold-thioglucose are resolved. Moreover, in the reconstructions obtained from sheets stained with the latter we could detect regions where uranyl acetate, acting as a positive stain, was incorporated into the particle. This may indicate that in these regions the RNA is concentrated and/or easily exposed to the stain. Regions which were stained by uranyl acetate could be located on the large subunits in their surface area which faces the internal empty space. Penetration of uranyl acetate to the region assigned as collar's ridge on the small subunits was also detected. In both cases the staining of these areas with uranyl acetate may stem either from the existence of exposed rRNA regions, as previously found [17] or from the presence of mRNA and tRNA in these locations.

Assignment of the known functional domains of the ribosomal subunits to the various structural features of our model still awaits further investigations. We hope that we shall be able to locate

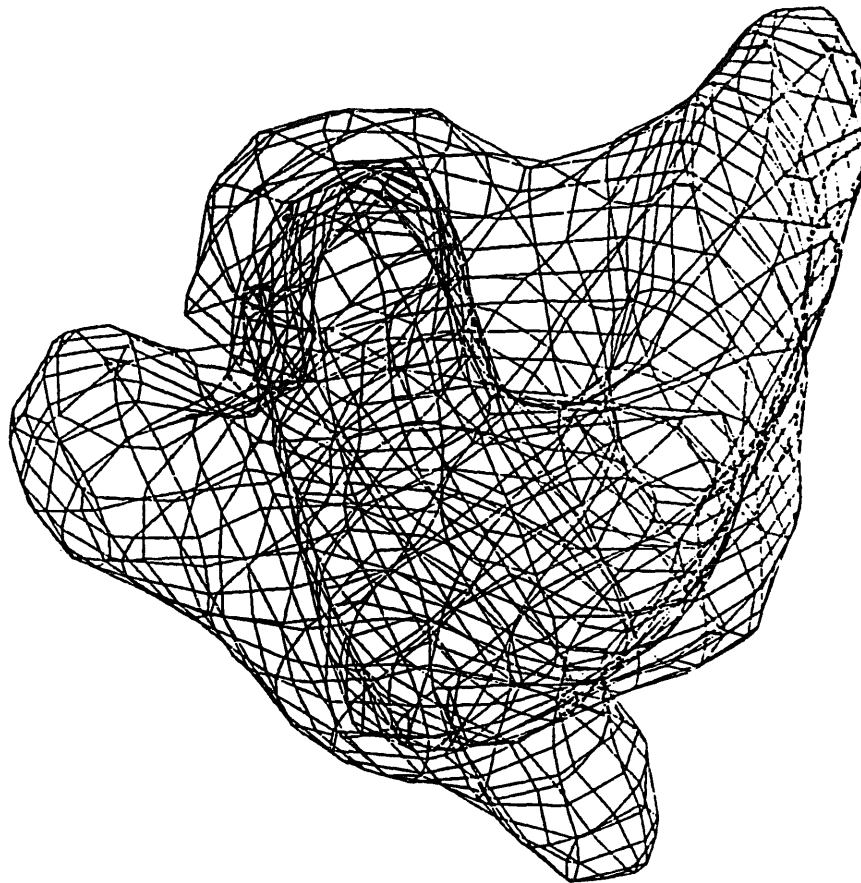


Fig. 4. Computer graphic display of the outline of the reconstructed model of the 50S ribosomal subunits [9].

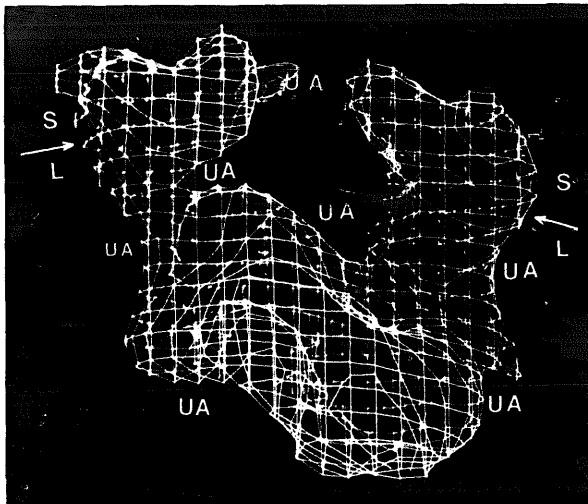


Fig. 5. Computer graphic display of the outline of the reconstructed model of the 70S ribosomes, obtained from sheets stained by uranyl acetate. Areas of substantial interaction with the stain are marked by (UA).

specific sites on a more detailed model in the foreseeable future.

### Acknowledgments

We thank K.R. Leonard and J.L. Sussman for their computer software, B. Shaanan and A. Levy for assistance with computer problems, C. Glotz, J. Müssig, B. Romberg and Y. Halfon for skillful technical assistance. This work was supported by NIH (GM34360), BMFT (05180 MPBO) and Minerva research grants.

### References

- 1 Makowski I., Frolov F., Saper M.A., Shoham M., Wittmann H.G. & Yonath Y. (1987) *J. Mol. Biol.* 193, 819–822
- 2 Yonath A., Bartunik H.D., Bartels K.S. & Wittmann H.G. (1984) *J. Mol. Biol.* 177, 201–206

- 3 Yonath A., Saper M.A., Makowski I., Müssig J., Piefke J., Bartunik H.D., Bartels K.S. & Wittmann H.G. (1986) *J. Mol. Biol.* 187, 633–636
- 4 Yonath A., Saper M.A. & Wittmann H.G. (1986) in: *Structure, Function and Genetics of Ribosomes* (Hardesty B. & Kramer G., eds.). Springer-Verlag, Heidelberg and New York, pp. 112–127
- 5 Yonath A., Saper M.A., Frolow F., Makowski I. & Wittmann H.G. (1986) *J. Mol. Biol.* 192, 161–162
- 6 Arad T., Leonard K.R., Wittmann H.G. & Yonath A. (1984) *EMBO J.* 3, 127–131
- 7 Wittmann H.G., Müssig J., Gewitz H.-S., Piefke J., Rheinberger H.J. & Yonath Y. (1982) *FEBS Lett.* 146, 217–220
- 8 Piefke J., Arad T., Gewitz H.S., Yonath A. & Wittmann H.G. (1986) *FEBS Lett.* 209, 104–106
- 9 Yonath A., Leonard K.R. & Wittman H.G. (1987) *Science* 236, 813–816
- 10 Amos L.A., Henderson R. & Unwin P.N.T. (1982) *Progr. Biophys. Molec. Biol.* 39, 183–231
- 11 Leonard K.R., Wingfiels P., Arad T. & Weiss H. (1981) *J. Mol. Biol.* 149, 259–274
- 12 Jones A. (1978) *J. Appl. Cryst.* 11, 268–272
- 13 Wittmann H.G. (1983) *Annu. Rev. Biochem.* 52, 35–65
- 14 Matthews B.W. (1968) *J. Mol. Biol.* 33, 491–497
- 15 Hogle J.M. (1982) *J. Mol. Biol.* 160, 663–668
- 16 Richmond T., Finch J.T., Rushton B., Rhodes D. & Klug A. (1984) *Nature* 311, 533–537
- 17 Milligan R.A. & Unwin P.N.T. (1986) *Nature* 319, 693–695